On-the-fly Classifying Sonar with Accurate Range and Bearing Estimation

Lindsay Kleeman

Intelligent Robotics Research Centre, Department of Electrical and Computer Systems Engineering
Monash University, Melbourne, Australia, Lindsay.Kleeman@eng.monash.edu.au

Abstract

This paper presents results from a four transducer pulse coded sonar system that performs target localisation in two dimensions and classification into planes, concave corners and convex edges whilst the sensor is in motion. On each sensing cycle two pulses are emitted from separate transmitters, and two receivers collect echoes that are processed using a DSP. The sensor achieves on-the-fly classification by transmitting nearly simultaneously from the two transmitters.

The effects of sensor motion are analysed in the paper and effects on range and bearing estimation can then be compensated using odometry based robot velocity measurements. Results are presented that show classification and angle measurement deviations from a robot moving at speeds up to 1 metre per second.

1 Introduction

Sonar classification provides a fast means for determining geometric properties of features in the environment surrounding a robot [1,2,4,5,6]. When the robot moves to a new position, the classification allows a prediction to be made of where the target will then appear. Sonar classification is usually based on discriminating targets into planes, convex edges and concave right-angled corners [1,2,4,5,6]. Sensing a known plane allows an immediate angular fix for the robot and constrains the position of the robot along a line parallel to the plane. Sensing known corner or edge target types, which are point features, constrain the robot position to a circle around the point feature with appropriate orientation on each position on the circle.

To date, sonar classification has been performed on stationary robots [1,2,4,5,6] or relies on assembling multiple sonar readings on a moving robot [7]. This paper presents new results that demonstrate single sensor cycle classification that is performed as the robot moves. This allows faster map formation and provides rapid, reliable data association on simultaneous localisation and mapping problems.

When sensing range and angle to a target from a moving platform with sonar, the measurements are affected by the velocity of the platform. This paper derives theoretical results that allow compensation for this motion. These results depend on the classification of the target and so it is therefore necessary to perform the classification in conjunction with ranging and bearing estimation on a moving robot.

The sonar classification technique relies on sensing the target from two transmitter positions. The approach used in this paper is to accurately control the time separation of the transmitter firings so that the identity of the transmitters can be retrieved from the echoes on the two receivers. Also this time separation is randomly varied from one sensor cycle to the next for two reasons. Firstly this enables interference rejection from other sonar systems, even identically configured, since we are looking for a precise time separation in the receivers. Secondly, pulse overlap problems due to awkwardly spaced targets are unlikley to recur in later sensing cycles. A typical transmitter firing separation ranges from 150 to 250 microseconds. A 200 microsecond separation corresponds to just 0.2 mm on a robot moving at 1 m/second. Two targets would need to be 34 mm apart to mimic 200 microseconds echo separation.

Using DSP technology we have produced a sensor that provides high range and bearing accuracy, implements a proven interference rejection method, and classifies multiple targets [1]. It does this all with a single sensing of the environment. The repetition rate depends on the number of pulses processed (clutter in the environment), and is typically 25 Hz.

This paper is organised as follows. The next section introduces the sonar system and the robot that are used in later experiments in section 6. Theoretical results of the effects on motion on sonar TOF and arrival angle are derived in Section 3. The effects of a moving observer on reception angle are derived in Section 4 and the results of sections 3 and 4 are combined and summarised in section 5. Experimental results are given in Section 6.

2 Four TOF Sensor

Only a brief description of the sonar sensor is given here since previous papers [1,2,3] describe the sensor. The sonar sensor is shown in Figure 1 and measures 150 x 100 x 70 mm. It is powered by a single 5 V supply and communicates with its host by a high-speed serial link. Two transmitters are mounted above two receivers, forming a square with only 40 mm between centres. Polaroid 7000 series transducers are deployed with their front grilles removed to reduce signal ringing.

As shown in Figure 2 the received signals are amplified, low pass filtered and digitised at 1 Mz and 12 bit precision, then processed with an Analog Devices 33 MHz ADSP2181. The DSP also generates the transmit waveforms and communicates with the host via an external UART.

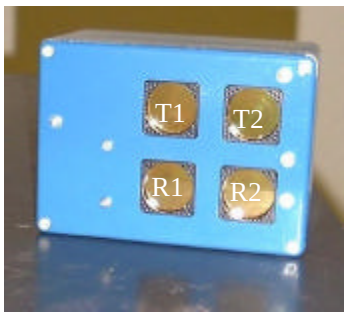

Figure 1*: DSP Sonar System with transmitters and receivers marked.*

A pulse is fired from the right transmitter first, and rapidly followed from the left with a randomly chosen 150 to 250 µs delay. This random delay provides the advantage of reducing the likelihood of cluttered environments producing pulse overlap problems on successive firings. Since the transmit time delay is sought out on the received data during DSP processing, interference can be rejected from neighbouring sonar systems running the same pulse scheduling algorithm at almost certainly a different synchronisation.

Echoes are digitised and processed on a DSP, yielding up to four arrival times for reflections from each target. The arrival times are grouped into tuples to allow classification of targets into planes, corners and edges, based primarily on the difference in arrival angles from the two transmitter's pulses. Due to the rapid succession of firing of the two transmitters, there is negligible movement possible between firing of the transmitters. For example at the top speed of our test robot shown in Figure 3 of 1 metre per second, a 200 microsecond transmitter pulse separation results in 0.2 mm movement. As shown in the experimental results, the sonar has been successfully tested for classifying targets at speeds up to 1 metre per second. The robustness of the classification at speed can be attributed to the fact that the difference in bearings to images of the transmitters is unaffected by motion.

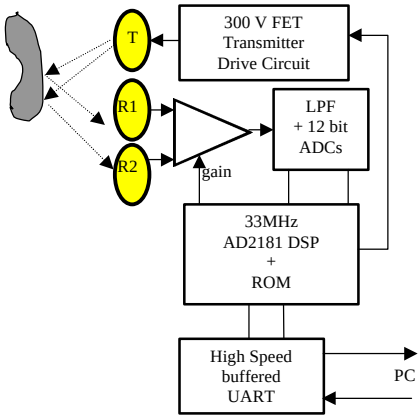

Figure 2:*:Hardware Block Diagram*

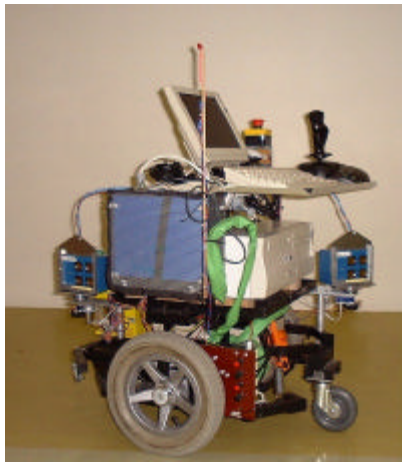

Figure 3: *Two DSP sonar sensors mounted panning mechanism on a mobile robot.*

3 Modelling Sensor Movement

In this section the effects of sensor velocity on the time-of-flight (TOF) and reception angle are analysed for the three cases of a plane, edge and corner target type. In all three cases, the point at which the sonar system transmits is labelled T and the displaced point of reception is R. The distance between T and R is *TOF*v*, where *v* is the magnitude of the velocity vector which is split into two orthogonal components v_x and v_y. The expressions derived in this section apply to any sonar sensor, since only the physics of sound propagation and reflection are utilised. The case of the plane target type is discussed first.

3.1 Plane Analysis

The geometry of the plane target reflecting the transmitted

pulse from T to R is shown in Figure 4. The TOF is broken up into two sections t_1 , representing the time to the plane and t_2, from the plane to the receiver R. The objectives of the analysis are to find the effect of the sensor velocity on the $TOF=t_1+t_2$ and the angle of reception, q, with respect to a stationary observer. The effect on the reception angle of a moving observer is discussed in the next section.

Notice that from the right-angled triangle formed by T and the distance d_1 from the plane, that

$$\sin q = \frac{t_1 v_x}{t_1 c} = \frac{v_x}{c} \tag{1}$$

$$\cos q = \sqrt{1-\left(\frac{v_x}{c}\right)^2} \tag{2}$$

where c is the speed of sound. For small velocities relative to c:

$$q = \sin^{-1}\left(\frac{v_x}{c}\right) \cong \frac{v_x}{c} \tag{3}$$

From the same triangle

$$\cos q = \frac{d_1}{t_1 c} \Rightarrow t_1 = \frac{d_1}{c\cos q} \tag{4}$$

From the right-angled triangle involving the reflected path to R:

$$\cos q = \frac{(t_1+t_2)v_y + d_1}{t_2 c} \Rightarrow t_2 = \frac{(t_1+t_2)v_y + d}{c\cos q} \tag{5}$$

Adding equations (4) and (5) and solving for $TOF=t_1+t_2$ with help from equation (2)

$$TOF = \left(\frac{2d_1}{c}\right)\frac{1}{\sqrt{1-\left(\frac{v_x}{c}\right)^2}-\frac{v_y}{c}} \tag{6}$$

Note that the first term in equation (6) represents the zero velocity solution for TOF and the second term represents the effect of non-zero velocity and is close to unity for small velocities compared to the speed of sound.

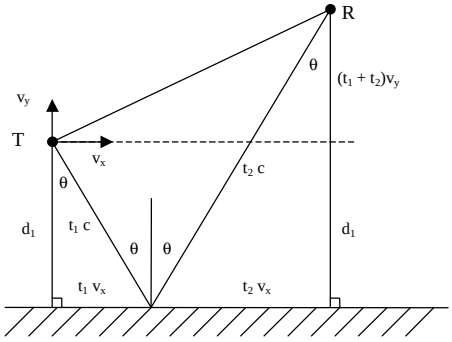

Figure 4: *Plane target with Sensor Movement*

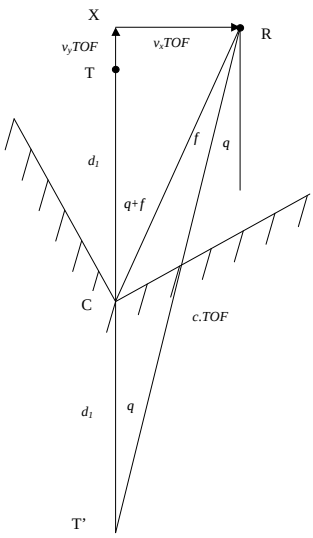

Figure 5: *Corner Geometry*

3.2 Corner Analysis

The geometry of the corner target reflecting the transmitted pulse from T to R is shown in Figure 5. The virtual image of T is shown as T' which is obtained by reflecting though both orthogonal planes of the corner, resulting in a reflection through the corner intersection point C.

Similar to the plane analysis, the objective is to find the motion altered TOF and reception angle discrepancy from the direction to the corner C, shown as f in Figure 5. Starting with the right-angled triangle T'XR

$$c^2 TOF^2 = \left(2d_1 + v_y TOF\right)^2 + v_x{}^2 TOF^2 \tag{7}$$

Solving equation (7) for TOF yields:

$$TOF = \frac{2d_1}{c}\left[\frac{\sqrt{1-\left(\frac{v_x}{c}\right)^2}+\frac{v_y}{c}}{1-\left(\frac{v}{c}\right)^2}\right] \tag{8}$$

where $v^2=v_x{}^2+v_y{}^2$. Note that the first term of (8) represents the zero velocity solution for the TOF and the second term represents the effect of velocity and is close to unity for small velocities compared to the c.

The angle f in Figure 5 represents the ground referenced angle deviation caused by the motion of the sonar sensor. This angle is now derived.

From the right-angled triangle T'XR

$$\tan q = \frac{v_x TOF}{2d_1 + v_y TOF} \tag{9}$$

and from triangle CXR

$$\tan(\theta+\phi)=\frac{v_x TOF}{d_1+v_y TOF} \tag{10}$$

From equations (9) and (10)

$$\frac{\sin(\theta+\phi)}{\cos(\theta+\phi)}=(2-k)\frac{\sin\theta}{\cos\theta} \tag{11}$$
$$where\ \ k=\frac{v_y TOF}{d_1+v_y TOF}$$

expanding the *sin* and *cos* sums and rearranging gives

$$\tan\phi=\tan\theta\left(\frac{1-\sin^2\theta}{\frac{v_y TOF}{d_1}+1+\sin^2\theta}\right) \tag{12}$$
$$=\left(\frac{v_x}{\frac{2d_1}{TOF}+v_y}\right)\left(\frac{1-\sin^2\theta}{\frac{v_y TOF}{d_1}+1+\sin^2\theta}\right)$$

For v_x, v_y<<c, sinθ<<1 and $\frac{2d_1}{TOF}\cong c$ and so equation (12) leads to the approximation

$$\phi\cong\frac{v_x}{c} \tag{13}$$

3.3 EdgeAnalysis

An edge re-radiates the transmitted ultrasound from a point source, and therefore the reception angle with respect to a stationary observer is unaffected by motion as shown in Figure 6. The TOF however is changed due to the new receiving position.

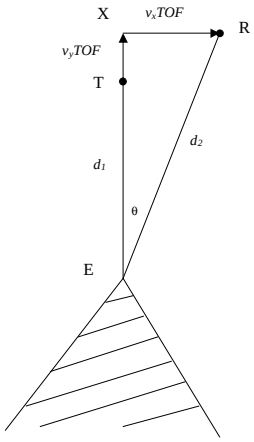

Figure 6: *Edge Geometry*

From the right-angled triangle XER

$$d_2{}^2=(d_1+v_y)^2+v_x{}^2TOF^2 \tag{14}$$

and also

$$d_1+d_2=cTOF \tag{15}$$

Solving equations (14) and (15) for the TOF yields

$$TOF=\frac{2d_1}{c}\left(\frac{1+\frac{v_y}{c}}{1-\frac{v^2}{c^2}}\right)\cong\frac{2d_1}{c}\left(1+\frac{v_y}{c}\right) \tag{16}$$

where the approximation in equation (16) is valid for v<<c.

4 Angle of Arrival Relative to the Moving Observer

The expressions for the reception angle in the previous section are based on an observer that is stationary with respect to the propagating medium, air. Suppose now the observer is moving at the same velocity as the sensor – which of course is the case in practice. Suppose a wavefront arrives at an angle α relative to air, as shown in Figure 7. The velocity components of the wavefront relative to the observer, w_x and w_y are as follows

$$w_x=c\sin\alpha-v_x \tag{17}$$
$$w_y=c\cos\alpha-v_y$$

therefore from equations (17) the observed angle of arrival, β is given by

$$\tan\beta=\frac{c\sin\alpha-v_x}{c\cos\alpha-v_y}=\frac{\sin\alpha-\frac{v_x}{c}}{\cos\alpha-\frac{v_y}{c}} \tag{18}$$

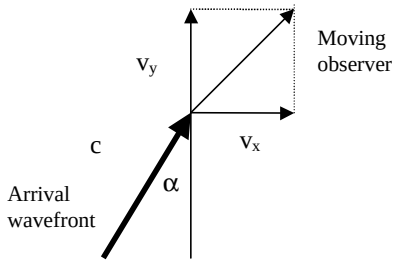

Figure 7: *Moving Observation of Wavefront*

5 Summary of Observed Approximate Arrival Angles

In this section, the previous results are approximated for speeds that can be expected on a mobile robot carrying the sonar sensor. The speed is assumed to be no more than a few metres per second – that is less than 1% of the speed of sound (typically 340 m/s at room temperature).

From equations (18) and (1), for a plane, the arrival angle relative to the sensor is exactly zero:

$$b_{PLANE} = \tan^{-1}\left(\frac{\frac{v_x}{c} - \frac{v_x}{c}}{\cos a - \frac{v_y}{c}}\right) = 0 \qquad (19)$$

This is no surprise when one realises that the wavefront follows a path relative to the moving sensor on a line seen to be perpendicular to the plane from the sensor's perspective. That is the wavefront forward velocity component is always the same as the sensor's due to reflection preserving this component.

The situation for a corner is quite different, since the angle f results in a wavefront that appears to come forward (*ie* displaced in the same direction as the sensor motion) from the real corner direction, as can be seen in Figure 5. The effect of the moving observer doubles this effect as seen by equations (18) and (13)

$$b_{CORNER} \cong \tan^{-1}\left(\frac{-\frac{v_x}{c} - \frac{v_x}{c}}{\cos a - \frac{v_y}{c}}\right) \cong -\frac{2v_x}{c} \qquad (20)$$

For the edge there is just the moving observer effect:

$$b_{EDGE} \cong \tan^{-1}\left(\frac{0 - \frac{v_x}{c}}{\cos a - \frac{v_y}{c}}\right) \cong -\frac{v_x}{c} \qquad (21)$$

6 Experimental Results

The mobile robot shown in Figure 3 was programmed to follow straight line paths, accelerating up to 1 m/sec in approximately 0.5 m and travelling for approximately 3 m before stopping. The sonar systems are mounted on active PID controlled panning mechanisms with angle encoder resolution of 0.18 degrees (0.003 radians). The results of tracking a wall in the laboratory with the front sonar are shown in Figure 8, where the robot position was derived from wheel odometry measurements. These results illustrate the ability of the sensor to perform on-the-fly classification of planes The wall angle did not vary discernibly with speed of the robot which is consistent with the theory derived for a plane in this paper. Moreover the sonar consistently classified the wall as a plane throughout the motion.

The robot performed a similar run at a speed of 1 m/sec whilst the front sonar tracked and classified a corner as shown in Figure 10. The sonar successfully classified the corner on almost all measurements, despite being near the limit of its range of 5 metres. This demonstrates the ability of the sonar sensor to perform on-the-fly classification of corners.

Figure 9 shows the deviation in angle as the robot moved. The theoretical angle deviation expected from the sonar motion of 1.0 metres per second is 0.006 radians. The results in Figure 9 are consistent with this deviation. Note that the robot starts at rest at a vertical distance x=0.3 and accelerates to 1 m/sec at x=0.8. The errors at x=3.2 can be attributed to the robot lurching as it stops abruptly. The sources of errors are:

- the panning encoder measuring the angle of the sonar. This has a resolution of 0.003 rad. that can result in maximum errors of at least 0.0015 rad.
- odometry errors which are reduced by travelling in a straight line.
- sonar measurement errors which are of the order of ±0.002 rad and vary in a correlated fashion with a time constant of several seconds [3].

Particular care was taken to eliminate a systematic cyclic odometry error. This error was due to small encoder misalignments and contributed approximately a 1 degree (0.017 radians) error that was sinusoidal with wheel angle. This error was removed by calibration of the robot odometry whilst travelling directly towards a wall and observing sonar angle measurements.

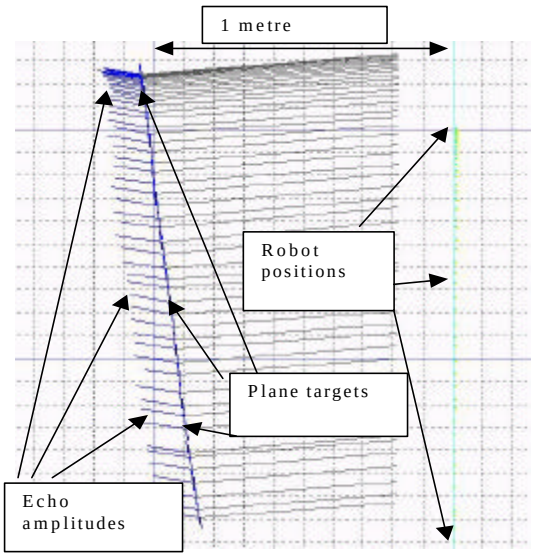

Figure 8: *Robot map from tracking and classifying a plane at a speed of 1 m/sec. The robot stops at the top.*

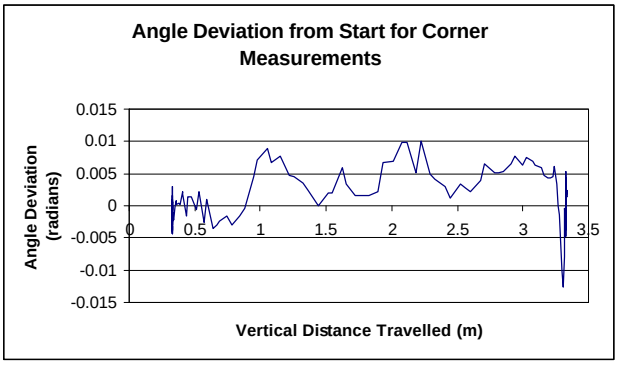

Figure 9: *Angle measurement error for the corner measurements shown in Figure 10.*

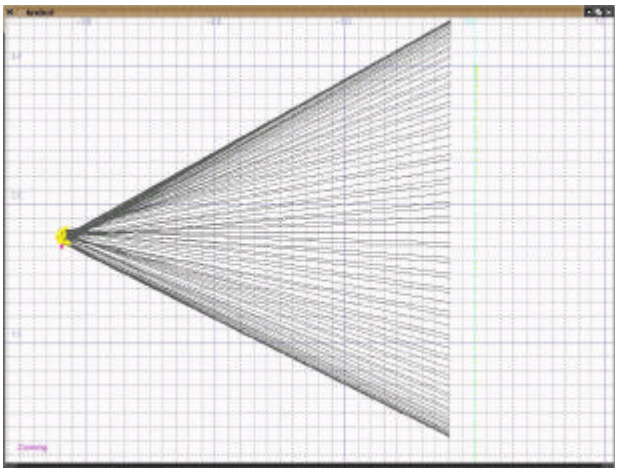

Figure 10: *Robot map from tracking and classifying a corner at 1 m/sec.*

7 Conclusions

This paper has derived important fundamental results for angle and range sonar sensing on a moving platform. The effects of motion on sonar angle and time of flight measurements are related to the robot speed normalised to the speed of sound. The effects are important in advanced sonar systems where angle measurement errors as low as 0.1 degrees have been reported [1,2].

Another outcome of this paper has been the demonstration that double pulse coded sonar systems [1] can reliably perform target classification whilst moving at least 1 metre per second. Previous generations of classifying sonar [2,5,4] were restricted to stationary sensing due to the comparatively long time between transmitter firings.

Future work will apply these results to rapid map building with the on-the-fly sonar systems. Modelling of errors of sonar measurements from moving platforms is an area of future interest.

Acknowledgements

The financial support of a Australian Research Council Discovery Project DP0210359, Large Grant A10017057 and the technical support of Steve Armstrong are gratefully acknowledged. DSP software development was assisted by Andrew Heale. Analog Devices are also acknowledged for donating DSP development systems through their University Program. This paper is dedicated to the memory of Teruko Yata who was an excellent sonar researcher and outstanding person.

References

[1] A. Heale and L. Kleeman, “Fast target classification using sonar” IEEE/RSJ International Conference on Intelligent Robots and Systems, Hawaii, USA October 2001, pp. 46-1451.

[2] L. Kleeman and R. Kuc, "Mobile robot sonar for target localization and classification", International Journal of Robotics Research, Vol 14, No 4, August 1995, pp 295-318.

[3] L. Kleeman, “Fast and accurate sonar trackers using double pulse coding”, IEEE/RSJ International Conference on Intelligent Robots and Systems, Kyongju, Korea, October 1999, pp 1185-1190.

[4] H. Peremans, K. Audenaert, and J. M. V. Campenhout, “A high-resolution sensor based on tri-aural perception,” IEEE Transactions on Robotics and Automation, Vol 9, pp 36-48, 1993.

[5] K S Chong and L. Kleeman, ”Feature-based mapping in real, large scale environments using an ultrasonic array”, International Journal Robotics Research, Vol 18, No 1, Jan 1999, pp 3-19.

[6] Hong Mun-Li and Lindsay Kleeman, “Ultrasonic classification and location of 3D room features using maximum likelihood estimation”, Robotica, Vol 15, pp 483-491 and 645-652, 1997.

[7] H. J. S. Feder, J. J. Leonard and C. M. Smith. “Adaptive mobile robot navigation and mapping” International Journal of Robotics Research, Vol 18, No 7, pp 650-668, 1999.